Photoproduction and relaxation of long-lived active charges in $Ca_3Mn_2Ge_3O_{12}$ garnet revealed through optical absorption

V. V. Eremenko, S. L. Gnatchenko, I. S. Kachur, V. G. Piryatinskaya, A. M. Ratner, and V. V. Shapiro
Institute for Low Temperature Physics & Engineering, National Academy of Sciences of Ukraine 61164 Kharkov, Ukraine
(Received 13 May 1999; revised manuscript received 20 October 1999)

Photoillumination causes an augmentation of optical absorption within the band corresponding to a forbidden transition. The observed kinetics of photoinduced absorption displays a broad continuous distribution of absorption centers over relaxation times, which cannot be explained, with allowance for the temperature dependence of the relaxation kinetics, in terms of absorption centers associated with impurities or lattice defects. The experimental picture, including its temperature changes, is described by the model of active charges (hole polarons) which arise under light pumping and produce random electric fields. These fields play a double role: they partly eliminate the forbiddenness of the optical transition, thus enhancing its oscillator strength, and significantly shorten the lifetime of active charges. A broad continuous distribution of random fields over magnitudes entails the corresponding lifetime distribution of active charges covering several orders of magnitude.

I. INTRODUCTION

During the last three decades, attention of researchers was drawn to a variety of magnetic insulator crystals, which are subject to photoinduced changes of optical and magnetic characteristics and at low temperatures retain the changed state after switching off illumination. The interest for such crystals has been kept largely due to alluring prospects to use them as active media in devices for high-density optical storage and optical processing of information.

For most of such magnetic insulators, e.g. $Y_3Fe_5O_{12}$, $EuCrO_3$, $FeBO_3$, α-Fe_2O_3, long-lived photoinduced phenomena are usually observed below the temperature of magnetic ordering. Persistent photoinduced changes, observed in a magnetically ordered state, involve interrelated optical and magnetic properties. For instance, in the case of yttrium iron garnet $Y_3Fe_5O_{12}$, illumination with linearly polarized light induces a change of magnetic anisotropy,[1–3] linear dichroism[3], and domain structure.[4] Unpolarized light affects magnetic permeability and susceptibility,[5,6] coercivity and mobility of domain walls,[7,8] magnetostriction[9], and optical absorption.[10,11] Interconnected variations in optical and magnetic properties make up a complicated physical picture. Due to this, the nature of persistent photoinduced phenomena in magnetic insulators up to now has been explored only in general features. For yttrium iron garnet[12,13] and other magnetic insulators,[14,15] these phenomena were usually associated with photoinduced charge transfer between lattice ions (including impurities). Jahn-Teller lattice deformation of ion surroundings, varying in the course of charge transfer, plays an important role in forming long-lived photoinduced changes.[16,17]

Unlike light-sensitive ferromagnets or ferrimagnets with a high Curie temperature, antiferromagnetic garnets with a low Neel temperature provide the possibility to separate persistent photoinduced changes of optical properties from those of magnetic characteristics related to a magnetically ordered state. For that purpose, the $Ca_3Mn_2Ge_3O_{12}$ garnet with the Neel temperature $T_N = 13.85$ K was investigated by the authors[16,18–20] in the temperature region $T_N < T < 200$ K where photoinduced phenomena were observed in the absence of magnetic ordering. Illumination of this crystal with linearly polarized light creates linear birefringence via redistribution of charges between orientationally nonequivalent octahedral positions (electrons are transferred from regular Mn^{3+} sites to Mn^{4+} ions present in the crystal in a small concentration due to a charged impurity or cation vacancies).[16,18–20] A rough estimate of this concentration follows from resonance studies of diluted garnets $Ca_3Ga_{2-x}Mn_xGe_3O_{12}$:[21,22] it was shown that the maximum concentration of Mn^{4+} in octahedral positions is of about 0.1 at. %, which corresponds to the concentration of Ge^{4+} vacancies in tetrahedral positions.

As was recently shown by the authors,[23] illumination of the garnet $Ca_3Mn_2Ge_3O_{12}$ with visible unpolarized light ($\lambda = 633$ nm) resulted in a noticeable increase (up to 15%) in the optical absorption coefficient at the same wavelength. In this case, the mechanism of charge transfer must act in another way since unpolarized light cannot redistribute charges between orientationally nonequivalent positions.

The aim of the present work is to elucidate the nature of light-induced optical absorption in the $Ca_3Mn_2Ge_3O_{12}$ garnet and to specify the role of photoinduced charge transfer. For that end, the kinetics of photoinduced absorption was studied in a broad range of light pumping intensities and temperatures, both under pumping and in the relaxation regime after switching off the pumping (Sec. II). Experimental picture exhibits unusual features, in particular, the existence of relaxation components with decay times distributed in a very broad interval.

These experimental data are explained in the subsequent Secs. III, IV, and V by a mechanism involving hole transfer in the Mn^{3+} sublattice. The holes are brought by light pumping to an active state where they produce random electric fields sufficient to enhance the oscillator strength of the forbidden optical transition. On the other hand, these fields pro-

mote hopping of holes in the Mn^{3+} sublattice which strongly shortens the lifetime of active charges. A broad continuous distribution of random fields over magnitudes entails the corresponding lifetime distribution of active charges covering several orders of magnitude.

II. EXPERIMENT

The sample in the form of a plane-parallel plate of the thickness $d \approx 35$ μm was cut from a single crystal of calcium-manganese-germanium garnet (CaMnGeG), was polished mechanically and then annealed at the temperature near 1000° C to eliminate internal stresses caused by polishing.

As it is known,[24–26] a twin domain structure arises in CaMnGeG at the temperature close to 520 K because of the Jahn-Teller phase transition from the cubic to tetragonal phase. Making allowance for this, a special thermal treatment[25] of the sample was carried out to increase the average size of the domains up to about 1 mm. A special sample holder with a diaphragm was used to select a single-domain region of the sample where the tetragonal axis was perpendicular to the plate surface. Thus, the results of the measurements are related to the sample with the tetragonal axis perpendicular to the surface. The sample was placed into a helium optical cryostat where temperature could be continuously varied from 2 to 300 K. The measurements were carried out in the temperature region $T \geqslant 23$ K above the Neel temperature. The sample temperature was controlled using a copper-constantan thermocouple.

The effect of illumination on the optical absorption of CaMnGeG was studied with the use of an optical double-beam set up. A helium-neon laser with the wavelength $\lambda = 633$ nm and the power of about 2×10^{-3} W (which corresponds to the photon flux 6×10^{17} cm^{-2} s^{-1}) was used as pumping source. The laser light had no fixed direction of polarization (it was partly polarized in a direction randomly varying with time). The stable wide-band emission of an arc xenon lamp, dispersed through a prism monochromator, served as probe light. Its intensity was sufficiently low to cause no photoinduced phenomena. The kinetics of the photoinduced augmentation of absorption was measured at the probe light wavelength 565 nm picked out by the monochromator. After passing through the sample, the probe light was run through a second monochromator to cut off the exciting light with the wavelength 633 nm and then was registered by a photomultiplier. Electric signal from the photomultiplier was amplified, transformed and transmitted to a computer for accumulation and analysis.

Prior to studying photoinduced variations in absorption, the transmission and reflection spectra of CaMnGeG were measured within the spectral interval $500 < \lambda < 800$ nm. The spectral measurements were carried out with the use of a prism monochromator with the linear dispersion 12 nm/mm at $\lambda = 500$ nm. The optical absorption spectrum of the garnet $Ca_3Mn_2Ge_3O_{12}$, obtained as a result of the measuring and usual processing of the transmission and reflection spectra, is shown in Fig. 1 (upper curve). As can be seen from the figure, the garnet is relatively transparent in the interval $650 < \lambda < 800$ nm but its optical absorption strongly increases with decreasing wavelength in the range $\lambda < 650$ nm. A very low transmission of the crystal for $\lambda < 650$ nm limited the measurement of spectrum from the high-frequency side.

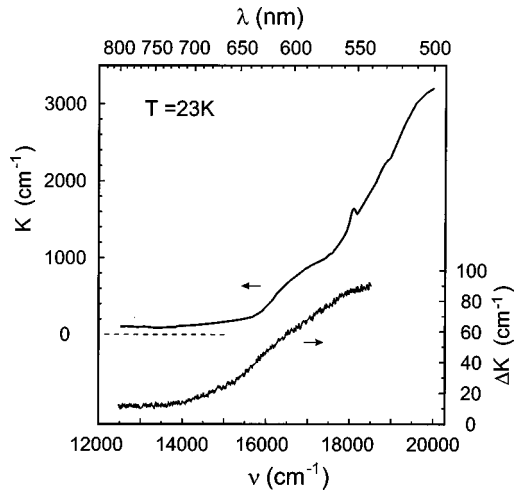

FIG. 1. Spectral dependence of the optical absorption coefficient (upper curve) and its photoinduced addition (lower curve) for the $Ca_3Mn_2Ge_3O_{12}$ garnet measured in the wavelength interval 500 to 800 nm at the temperature T=23 K.

Such spectral dependence of absorption, strongly growing with decreasing wavelength below 650 nm, can be attributed to a wide band with the maximum near 500 nm which is usually present in the optical spectra of compounds with Mn^{3+} and is related to the optical transition ${}^5E_g \rightarrow {}^5T_{2g}$ in the Mn^{3+} ion.[27,28] In the case of the $Ca_3Mn_2Ge_3O_{12}$ garnet, where a Mn^{3+} ion occupies an octahedral position, its orbitally degenerate states ${}^5E_g$ and ${}^5T_{2g}$ are split by the tetragonal distortion of oxygen octahedrons caused by the Jahn-Teller effect.[24] However, the splitting components of both the states retain their *g*-symmetry, so that the optical transition ${}^5E_g \rightarrow {}^5T_{2g}$ is forbidden in the dipole approximation. The corresponding absorption is reduced by four orders of magnitude compared to an allowed transition.

Illumination of the sample with laser light caused a change of the transmission spectrum in the examined region. Under illumination, the transmission of the CaMnGeG sample noticeably decreased, whereas no variation in the reflection coefficient R was registered within the interval $500 < \lambda < 800$ nm. Thus, the decrease in transmission, observed in this spectral region, should be assigned only to a light-induced enhancement of optical absorption. This permits one to derive the photoinduced addition to absorption coefficient, ΔK, from the transmitted light intensity j in a simple form

$$\Delta K = d^{-1} \ln(j_0 / j), \tag{1}$$

where j_0 and j is the intensity of the transmitted probe beam before illumination and after illumination, respectively. Figure 1 (lower curve) shows the spectral dependence of the photoinduced addition to absorption coefficient. It can be seen that absorption coefficient (upper curve) and its photoinduced addition have similar spectral dependences. This makes up grounds to attribute the initial absorption and its photoinduced augmentation to the same optical transition. Such suggestion underlies the further analysis (see Secs. III to V) and is corroborated by its results.

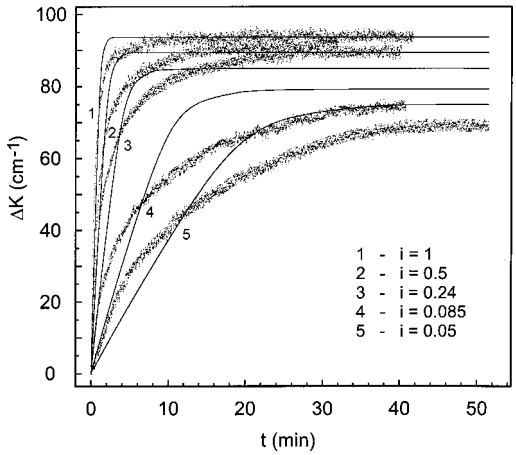

FIG. 2. Time dependences of the light-induced addition, Δ K,to the optical absorption coefficient of the $Ca_3Mn_2Ge_3O_{12}$ garnet measured at the wavelength 565 nm and $T=23$ K under laser irradiation with different intensities *i* (given in units of the maximal pumping intensity). Experimental data are plotted by dots; solid lines show the solution of kinetic Eq. (12).

Figure 2 demonstrates the observed time dependences of the photoinduced addition, $\Delta K(t)$, to absorption coefficient at $\lambda=565$ nm under irradiation with different intensities *i*. It can be seen from the figure that the photoinduced effect saturates after a time interval decreasing with an increase of light pumping *i*. The level of saturation, $\Delta K(\infty)$, depends on *i* but tends to a finite limit with an increase of *i*.

The saturation value of photoinduced absorption decreases with increasing temperature. This can be seen from Fig. 3 where the time dependences $\Delta K(t)$ at different temperatures are presented. The curves were measured for $\lambda=565$ nm and $i=1$ (the maximal pumping). Note that light-induced absorption in CaMnGeG is not observed when the sample temperature exceeds 190 K.

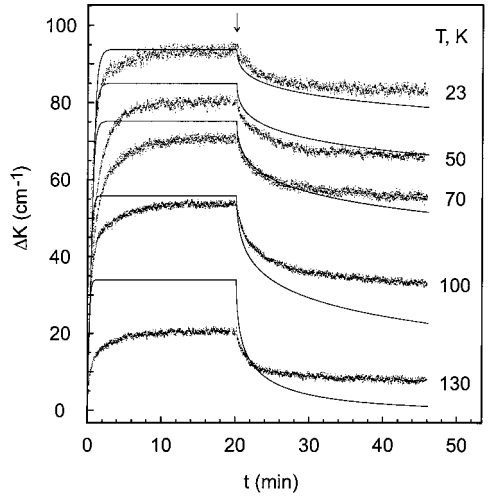

FIG. 3. Time dependences of the light-induced addition, Δ K, to the optical absorption coefficient measured at the wavelength 565 nm and different temperatures ($T=23$, 50, 70, 100, and 130 K) under pumping with the maximal intensity ($i=1$) and after switching off the pumping. Experimental data are plotted by dots; solid lines show the solution of kinetic Eq. (12). The moment of switching off illumination is indicated by arrow.

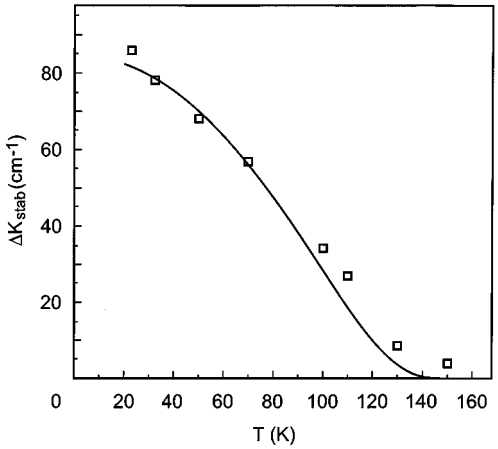

FIG. 4. Temperature dependence of the stable contribution, ΔK_{stab}, to photoinduced absorption defined as the ordinate of the corresponding relaxation curve, given in Fig. 3, at the moment $t=25$ m in after switching off illumination. Points denote experimental data; solid line gives the results of solving the kinetic Eq. (12).

In order to explore the relaxation of photoinduced absorption, the time dependences of ΔK were measured upon switching off light pumping. Figure 3 presents the photoinduced addition to absorption measured after switching off irradiation (this moment is indicated by arrow). Attention should be paid to the fact that the slope of each relaxation curve is significant immediately after switching off irradiation and drastically diminishes with time. Thus, there exists a practically stable residual contribution, ΔK_{stab}, to photoinduced absorption. At 23 K ΔK_{stab} amounts to about 90% of the initial ΔK value. With an increase of temperature, ΔK_{stab} decreases fast and monotonically as shown in Fig. 4.

III. MODEL OF FORBIDDEN OPTICAL TRANSITIONS ENHANCED BY RANDOM ELECTRIC FIELDS

Photoinduced electronic processes, resulting in an additional absorption, can be reconstructed with taking into account the main features of the experimental picture:

First, optical centers, responsible for photoinduced absorption, have a very broad distribution over relaxation time τ (defined from the relaxation curve slope). As seen from Fig. 3, this distribution covers the interval from a minute to several hours, the contribution of the most long-lived centers being predominant at low temperatures.

Second, the photoinduced addition to absorption $\Delta K(t)$ (presented in Fig. 2) saturates with exposition time to the stationary level $\Delta K(\infty)$ which tends to a finite limit with increasing intensity of pumping. The saturation time (about 2 min for the maximal pumping) does not correspond to relaxation time τ, which exceeds several hours for the predominant part of photoinduced centers (90% at 23 K). It follows that the saturation phenomenon cannot be immediately associated with their relaxation. It cannot be ascribed either to a decreasing dependence of τ on the number of photoinduced centers. Indeed, special measurements showed that the slope of the relaxation curve practically did not depend on the level of photoinduced absorption at the moment of switching off illumination (no matter how this level was given: by the

intensity or duration of pumping).

The model of photoinduced absorption must explain this nontrivial experimental picture. For that end, two alternative models (a) and (b) should be considered:

Model (a). Photoinduced addition to absorption is caused by some absorption centers different from Mn^{3+} ions and associated with impurities or lattice defects. This model should be discarded for the following reason. Photoinduced absorption centers, responsible for the observed relaxation picture (Fig. 3), have relaxation times $\tau_1, \tau_2, \ldots$, in the interval from 2 min to several hours. As temperature rises, the times τ_j strongly shorten (which follows from the diminution of photoinduced absorption), whereas the shape of the relaxation curve varies rather weakly and the stable part of photoinduced absorption centers decreases monotonically (Fig. 4). This means that with increasing temperature all relaxation components move to the left on the τ-axis with almost equal rates, every one of them being replaced by the nearest component with a longer τ . Such a regular distribution of absorption centers over τ , existing in a broad temperature interval, is highly improbable if they are associated with impurities or lattice defects.

Model (b). Photoinduced augmentation of absorption is associated with the same Mn^{3+} ions and the same forbidden optical transition ${}^5E_g \rightarrow {}^5T_{2g}$ between even states which are responsible for absorption in the absence of illumination. Photoillumination creates (in a way considered below) electric field which partially eliminates forbiddenness from this transition via creating an odd addition to an even state. Since this addition depends on energy, the spectrum of the photoinduced augmentation of absorption generally deviates from the initial spectrum but is confined within its boundaries and in the main reproduces its shape, as seen from Fig. 1. This similarity corroborates the model (b). Below this model will be developed in detail; as will be shown, it can naturally explain all experimental regularities.

The Mn^{3+} sublattice of the $Ca_3Mn_2Ge_3O_{12}$ garnet contains Mn^{4+} ions (i.e., Mn-holes) in a small concentration.[21,22] Since the crystal as a whole must be electrically neutral, it contains negative impurity ions or cation vacancies in the same concentration (for brevity we will speak about impurity ions with unit effective charge). In the ground state, Mn-holes occupy Mn-sites, adjacent with negative impurity charges, and form coupled pairs — dipoles of the length of a few Angstroms. Under photoillumination, a small number of electrons are transferred from regular Mn^{3+} ions to Mn^{4+} ions coupled with negative impurities, thus creating pairs of spatially separated charges of opposite signs (active charges). This process is schematically shown in Fig. 5. The fields of active charges enhance the forbidden optical transition by a quantity proportional to their number N.

On the other hand, random electric fields of active charges accelerate the hopping of holes between Mn ions and, hence, the recombination of holes with negative impurity charges (i.e., the formation of inactive coupled pairs). Below it is assumed that the hole lifetime, τ, relative to such recombination is proportional to the reciprocal rate of hole hopping between Mn^{3+} ions. A deviation from this proportionality will be discussed in Sec. V.

Consider now the probability of hole hopping from the ion A, where it stays in a polaronic state, to another ion B.

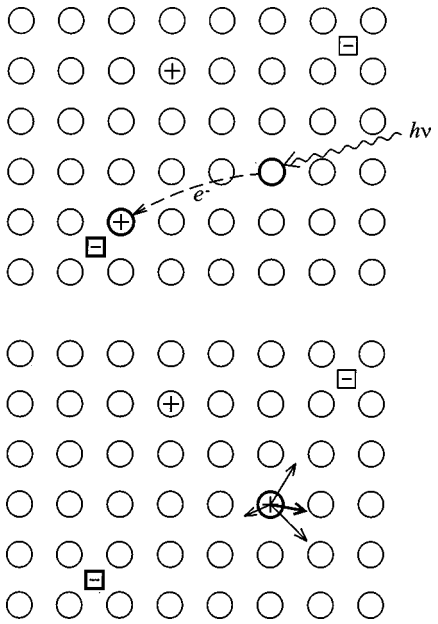

FIG. 5. Photoinduced transformation of a coupled pair of charges (indicated by bold square and circle) to a pair of dissociated active charges. Squares denote impurity ions, empty circles are regular Mn^{3+} sites and circles with ''plus'' are Mn^{4+} ions. Above: Initial picture to be changed by the photoinduced electron transfer (shown by dashed arrow) from a regular Mn^{3+} site to the Mn^{4+} ion coupled with a negative impurity. Below: The same after this electron transfer. The new active Mn^{4+} ion is indicated by bold circle. Thin arrows show random electric fields produced by the rest of active charges. The resulting field (bold arrow) generally does not coincide with the direction to the nearest impurity so that the active charge recombination is preceded by its complicate diffusion motion.

First, electric field is put equal to zero. The total energy of the hole polaron depends on the displacements, x_n, of atoms adjacent with the ion A

$$E_{\text{tot}} = -\sum_n C_n x_n + \sum_n K_n x_n^2/2$$

$$\equiv -\Delta_0 + (1/2)\sum_n K_n (x_n - x_{0n})^2,$$

$$\Delta_0 \equiv (1/2)\sum_n C_n^2/K_n . \qquad (2)$$

The polaron energy (2) consists of the electronic part, linear in displacements x_n, and the lattice deformation energy quadric in displacements. Δ_0 stands for the energy gap between the polaronic levels before hopping (at the site A with deformed surroundings) and after hopping (at the site B with undeformed surroundings). Electric field F diminishes this gap down to the value $\Delta(F) = \Delta_0 - Fea$ where a is the distance between adjacent Mn-sites, e is the free electron charge. The A-to-B hopping of the hole becomes possible if this gap is overcome by sufficiently strong fluctuations of the surroundings of the sites A and B. The hopping probability is expressed through the mean squared displacement of atoms from their equilibrium positions which is proportional, by definition, to the effective temperature T_{eff}. Finally, the rate

of active charge recombination, proportional to the *A*-to-*B* hopping rate, takes up the form

$$\Gamma(F)=\Gamma_0\exp(-\Delta_0/4T_{\rm eff}+Fea/2T_{\rm eff}). \tag{3}$$

In the Debye approximation,

$$T_{\rm eff}=(2T^2/\hbar\omega_D)\int_0^{\hbar\omega_D/2T} x\coth x\,dx, \tag{4}$$

with the Debye frequency ω_D. Effective temperature (4) coincides with the true temperature T at high temperatures and allows for zero vibrations of the lattice at low temperatures.

Equation (3) should be complemented by the distribution of the electric field **F**, produced by active charges, over magnitude:

$$P(F)=(3^{3/2}\beta^{3/2}\epsilon^3/2^{5/2}\pi e^3N^2)F^2 \times\exp(-3F^2\epsilon^2\beta/8\pi e^2N^{4/3}),$$

$$\beta\cong 0.071. \tag{5}$$

Here N is the number of active charges per unit volume and $\epsilon\approx 3\epsilon_0/(3+\epsilon_0)\approx 1.8$ is effective permittivity (ϵ_0 is the static permittivity of the crystal). This distribution function is written in a usual way for the magnitude of the field vector **F** presented as the sum of random fields produced by a large number of active charges.

IV. KINETIC EQUATION FOR ACTIVE CHARGES

Active charges are divided into groups, n_j, by their lifetime $\tau_j=\Gamma_j^{-1}$. The F-axis is divided into M intervals ΔF_j (with centers at the points F_j) in the way providing equal probabilities for an active charge to get into every interval ΔF_j at the moment of its generation:

$$\int_0^{F_j}P(F)dF=(j-0.5)/M,\quad \Delta F_jP(F_j)=1/M,$$

$$j=1,\ldots,M, \tag{6}$$

where the function (5) is used. For an active charge of the jth group, recombination rate is given by Eq. (3) with $F=F_j$.

Light pumping takes away J electrons per unit time from regular Mn^{3+} ions, thus enhancing (in the way shown in Fig. 5) the number of active charges in the jth group by the value J/M. These electrons are transferred either to active Mn^{4+} ions [with the probability $p=p(N)$] or to Mn^{4+} ions coupled with negative impurities (with the probability $1-p$). In the former case, the jth group population n_j decreases by a value proportional to the product $p(N)n_j$. Thus, the kinetic equation for the populations n_j is of the form

$$dn_j/dt=J[1/M-p(N)n_j/N]-\hat\Gamma n_j. \tag{7}$$

Here, $\hat\Gamma$ stands for the recombination operator, which in a rough approximation can be identified with the recombination rate (3) of an active charge at the moment of its generation.

The kinetic Eq. (7) explains the experimental regularities, summarized at the beginning of Sec. III, which cannot be understood within the conventional notion:

First, the lifetime distribution of active charges, given by Eqs. (3), (5), and (6), is continuous and covers a range of several orders of magnitude.

Second, even for very large lifetimes of active charges, the kinetic Eq. (7) describes the saturation of the number of active charges with increasing exposition time or pumping intensity. Indeed, for $\tau_j=\infty$ Eq. (7) after summing over j takes up the form $dN/dt=J[1-p(N)]$. As N increases, $p(N)$ grows and nears unity, so that dN/dt turns to zero. Let us introduce the characteristic saturation value, N_0, of the number of active charges at which its growth rate is half slowed down

$$p(N_0)=0.5. \tag{8}$$

Note that N_0 is much less than the number of inactive coupled pairs $N_{\rm coup}$: $N_0\ll N_{\rm coup}$. Indeed, at $N=N_0$ the total probability of electron trapping by any active charge is equal to that of electron trapping by any coupled pair. But the trapping section of an active charge is much greater since it creates a much stronger electric field than a coupled pair. The total number of coupled pairs must correspondingly exceed that of active charges.

To compare quantitatively the theory with experiment, it is necessary to specify the recombination operator $\hat\Gamma$ and probability $p(N)$ appearing in Eq. (7). In view of a complicate character of the corresponding physical processes, this is made below in a model way.

At the moment of its generation, an active charge of the jth group has recombination rate (3) with $F=F_j$. After that, the recombination rate of this charge varies due to the electric field variation caused by the disappearance and generation of other active charges at random points. The random field F and the corresponding recombination rate of the active charge are essentially varied when a significant part of other active charges is replaced by new generated charges. The fraction of new active charges, generated during the time dt, is $Jdt/N(t)$. This quantity, integrated over time, can serve as the measure of the corresponding change in the argument of Γ_j. Within the model, this is allowed for through the shift in the argument of the monotonically growing sequence $\Gamma_j(j=1,\ldots,M)$

$$\hat\Gamma n_j=n_j\Gamma_{j+Ms},\quad s(t)=\int_0^t Jdt/N(t) \tag{9}$$

(the definition $\Gamma_j=\Gamma(F_j)$ is extended with the period M).

Consider now the probability p for an electron, taken away by pumping from a Mn^{3+} ion, to be captured by one of the positive active charges. This takes place if the electron is separated from the nearest active charge by the distance r meeting the inequality $F_{\rm act}\equiv e/\epsilon r^2>F_{\rm bac}$. This condition means that the field, $F_{\rm act}$, of the active charge exceeds in magnitude the background field of coupled pairs $F_{\rm bac}$. The quantity $F_{\rm bac}^2$ can be estimated as the squared field of the dipole **d**, $F_0^2=2Zd^2/R^6\epsilon^2$, averaged over its orientations and multiplied by the coordination number $Z\approx 12$ ($R=N_{\rm coup}^{-1/3}$ is the mean distance between the dipoles). Thus, the condition of electron trapping by an active charge takes up the form

$$r<r_0, \quad r_0\equiv(24)^{-1/4}(aN_{\rm coup})^{-1/2}. \tag{10}$$

The condition (10) is not met only if *no one* of *NV* active charges, randomly situated in the crystal volume *V*, is found inside the spherical volume $V_0=(4/3)\pi r_0^3\ll V$. The probability for *one* active charge to be found outside the sphere is $1-V_0/V$; for *NV* charges this quantity should be raised to the power *NV*, resulting in $\exp(-NV_0)$. Thus, the probability for the condition (10) to be fulfilled is

$$p(N)=1-\exp(-NV_0)=1-\exp[-(4/3)\pi Nr_0^3], \tag{11}$$

where r_0 is defined by Eq. (10).

Equations (8) and (11) give the characteristic number of active charges per unit volume $N_0=1.8(aN_{\rm coup})^{3/2}$, which meets the inequality $N_0\ll N_{\rm coup}$.

The kinetic Eq. (7), after substituting Eqs. (9) and (11), takes up the form

$$d\nu_j/dt=I[1/M-(1-2^{-\nu})\nu_j/\nu]-\nu_j\Gamma_{j+Ms(t)},$$

$$s(t)\equiv\int_0^t Idt/\nu(t), \tag{12}$$

where *I* is pumping intensity in some units and the number of active charges is expressed in units of N_0

$$\nu_j=n_j/N_0, \quad \nu=\sum_j \nu_j=N/N_0. \tag{13}$$

V. COMPARISON OF THE THEORY WITH EXPERIMENT

The problem under consideration is specified by the following physical parameters:

The molar concentration, $a^3N_{\rm coup}$, of negative impurity ions which form coupled pairs of charges in the ground state. The corresponding molar concentration of active charges is $1.8\nu(a^3N_{\rm coup})^{3/2}$. These parameters specify the distribution function (5) of electric fields.

The depth, Δ_0, of the deformation potential well of a Mn-hole polaron.

The Debye frequency ω_D which specifies effective temperature (4) and together with parameters Δ_0 and preexponential Γ_0 determines the recombination rate (3) as a function of temperature.

The proportionality coefficient between *N* and $\Delta_0 K$ as well as that between *I* and experimental pumping intensity *i* are chosen as fitting parameters.

The solution of the kinetic Eq. (12) is best fitted with the total set of experimental data at the following values of parameters: $\Delta_0=1.08$ eV$=12500$ K, $\omega_D=0.035$ eV $=400$ K, $\Gamma_0=7\times10^5 s^{-1}$. The characteristic molar concentration of active centers N_0a^3 is equal to 0.2%, and its saturation value, achieved under full pumping ($i=1$), amounts to 0.08%. The corresponding molar concentration of the coupled pairs of charges is 1%.

These values of parameters seem reasonable for a solid. In particular, active charges of the given concentration create electric field of about 1.5×10^6 V/cm which is roughly 300 times less than intraatomic field and creates the oscillator strength of about 10^{-5} for a forbidden transition. In the visible range this corresponds to the absorption coefficient of the scale of 100 cm^{-1}, in a qualitative agreement with experiment. Rather a large depth of the polaronic potential well ($\Delta_0=1.08$ eV) should be associated with the Jahn-Teller lattice deformation changing when Mn-hole hopping.

For the given values of parameters, the solution of the kinetic Eq. (12) is shown by solid lines in Figs. 2 to 4. The figures demonstrate a qualitative agreement of the theory with experiment within broad ranges of temperature and pumping, both under pumping and after switching off the pumping.

In the latter case, the calculated relaxation rate systematically exceeds the experimental one. The reason of this discrepancy is rather obvious: The relation (3), used when solving the kinetic equation, implies that the recombination rate, Γ, of an active charge *A* is proportional to the probability of its jump to an adjacent Mn^{3+} site. In fact, however, Γ depends also on the distance, *R*, of the charge *A* from the nearest negative charge: Γ fast decreases with increasing *R*. Equation (3) gives a small Γ for a charge *A* if random field at the point *A* is weak, that is no other charges are in its vicinity; but in this case *R* is large and, hence, the true recombination rate must be significantly less than the hopping rate (3). Thus, for a small Γ the model overestimates relaxation rate; in other words, the length of tails of the calculated relaxation curves, presented in Fig. 3, is underestimated.

Attention should be drawn also to another discrepancy between the theory and experiment shown in Fig. 3. As can be seen from the figure, the experimental time dependences of photoinduced absorption under pumping, measured at various temperatures, exhibit two characteristic times t_1 and $t_2\gg t_1$. First absorption fast grows during the time $t_1\cong2$ min., but this fast growth stops at the level $\Delta K(\infty)-K_1$ near the complete saturation level $\Delta K(\infty)$ $[K_1\ll\Delta K(\infty)]$. After that, absorption achieves complete saturation much slower, with the characteristic time $t_2\cong10$ min.

The theory describes only the fast process. The slow process can be associated with deep hole traps (probably, Mn^{3+} ions positioned in the vicinity of some lattice defects). Initially the traps are empty and neutral, but after filling in by holes they begin to act as stable active charges with an infinite recombination time τ (a pinned hole cannot recombine with a pinned negative charge). At low temperatures the contribution of trapped holes to the photoinduced absorption amounts to about 10%; hence, their concentration is ten times less than the total concentration of active charges and amounts to $c_{\rm tr}\cong2\times10^{-4}$. Due to their low concentration, the traps are slowly filled in which explains a large characteristic time t_2.

The contribution of filled traps to absorption, presented in Fig. 3 by the experimental curves, can be satisfactorily described in the exponential form

$$\Delta K_{\rm tr}(t)=K_1[1-\exp(-t/t_2)] \tag{14}$$

with parameters almost constant in the temperature range $T\leqslant100$ K: $K_1\cong10$ cm^{-1} and $t_2\cong7$ min. At $T=T_1=130$ K, K_1 diminishes roughly two times. This permits one to estimate the trap depth as $T_1\ln(1/c_{\rm tr})\cong1100$ K$=0.1$ eV.

VI. CONCLUSION

Experiment displays a broad distribution of photoinduced absorption centers over relaxation times and the saturation of photoinduced absorption with time and pumping intensity. Such experimental regularities cannot be explained in terms of absorption centers associated with impurities or lattice defects.

This experimental picture is naturally explained within the model of random electric fields created by Mn-holes (Mn^{4+} ions). In the ground state these holes are inactive: they are coupled with pinned negative charges (impurity ions or cation vacancies) and produce a weak electric field. Light pumping brings the holes in an active (dissociated) state, thus strongly enhancing their field, via transferring electrons from regular Mn^{3+} ions to Mn^{4+} ions coupled with the negative charges. Electrons are partially transferred also to active charges (Mn^{4+} ions) resulting in annihilation of active charges. The rate of their annihilation increases with the number of active charges, which entails its saturation with an increase of exposition time or pumping intensity. The photoinduced absorption, observed within the band corresponding to a forbidden optical transition, is produced by active charges: their electric field partially eliminates the forbiddenness and enhances the optical transition.

On the other hand, the random electric fields of photoinduced active charges promote their hopping in the Mn^{3+} sublattice and recombination (coupling) with pinned negative charges; a broad distribution of random fields over magnitudes gives rise to a very broad range of lifetimes of Mn holes relative to recombination with negative charges.

The model of random electric fields describes the total set of experimental data: time dependence of photoinduced absorption ΔK under pumping and during relaxation as well as the dependence of ΔK on pumping intensity and temperature. The model gives an estimate for the concentration of active charges near 0.1 mol. %, which corresponds to the quantum yield of their creation on the initial linear stage of about 10^{-3}.

ACKNOWLEDGMENTS

The authors are thankful to Dr. J.-M. Desvigness (CNRS Laboratoire de Physique des Solides, Meudon-Bellevue, France) for providing $Ca_3Mn_2Ge_3O_{12}$ single crystals. This research was partly supported by the INTAS Grant Nos. 96-626 and 97-366.

[1] R.W. Teale, and D.W. Temple, Phys. Rev. Lett. **19**, 904 (1967).
[2] R.F. Pearson, A.D. Annis, and P. Kompfner, Phys. Rev. Lett. **21**, 1805 (1968).
[3] J.F. Dillon, E.M. Gyorgy, and J.P. Remeika, Phys. Rev. Lett. **23**, 643 (1969).
[4] V.F. Kovalenko, E.S. Kolezhuk, and P.S. Kuts, Zh. Éksp. Teor. Fiz. **81**, 1399 (1981) [Sov. Phys. JETP **54**, 742 (1981)].
[5] K. Hisatake, K. Ohta, N. Ichinose, and H. Yokoyama, Phys. Status Solidi A **26**, K75 (1974).
[6] M. Pardavi-Horvath, P.E. Wigen, and G. Vertesy, J. Appl. Phys. **63**, 3110 (1988).
[7] H. Van der Heide, and U. Enz, Solid State Commun. **6**, 347 (1968).
[8] W. Lems, R. Metselaar, P.J. Rijnierse, and U. Enz, J. Appl. Phys. **41**, 1248 (1970).
[9] V.G. Veselago, N.V. Vorob'ev, and R.D. Doroshenko, Pis'ma Zh. Éksp. Teor. Fiz. **45**, 402 (1987) [JETP. Lett. **45**, 512 (1987)].
[10] E.M. Gyorgy, J.F. Dillon, and J.P. Remeika, J. Appl. Phys. **42**, 1454 (1971).
[11] K. Hisatake, I. Matsubara, K. Maeda, H. Yasuoka, H. Mazaki, and K. Vematsu, J. Magn. Magn. Mater. **140–144**, 2127 (1995).
[12] R. Alben, E.M. Gyorgy, J.F. Dillon, and J.P. Remeika, Phys. Rev. B **5**, 2560 (1972).
[13] M. Wurlitzer and J. Franke, Phys. Status Solidi A **64**, 539 (1981).
[14] G.S. Patrin, N.V. Volkov, and G.F. Petrakovskii, Fiz. Tverd. Tela (Leningrad) **36**, 1385 (1994).
[15] G.S. Patrin, D.A. Velikanov, and G.F. Petrakovskii, Fiz. Tverd. Tela (Leningrad) **37**, 1214 (1995).
[16] S.L. Gnatchenko, V.V. Eremenko, S.V. Sofroneev, and N.F. Kharchenko, Pis'ma Zh. Eksp. Teor. Fiz. **38**, 198 (1983) [JETP Lett. **38**, 233 (1983)].
[17] Yu.V. Fedorov, F.F. Leksikov, and F.T. Aksenov, Zh. Éksp. Teor. Fiz. **89**, 2099 (1985).
[18] S.L. Gnatchenko, N.F. Kharchenko, V.A. Bedarev, V.V. Eremenko, M. Artinian, J.-M. Desvignes, and H. Le Gall, Fiz. Nizk. Temp. **15**, 627 (1989) [Sov. J. Low Temp Phys. **15**, 353 (1989)].
[19] V.A. Bedarev and S.L. Gnatchenko, Fiz. Nizk. Temp. **20**, 124 (1994) [J. Low Temp. Phys. **20**, 100 (1994)].
[20] B. Sugg, S.L. Gnatchenko, and R.A. Rupp, J. Opt. Soc. Am. B **13**, 2662 (1996).
[21] A.E. Nosenko, B.V. Padlyak, and V.V. Kravchshin, Fiz. Tverd. Tela (Leningrad) **27**, 3455 (1985).
[22] B.V. Padlyak and A.E. Nosenko, Fiz. Tverd. Tela (Leningrad) **30**, 1788 (1988).
[23] V.A. Bedarev, S.L. Gnatchenko, R.A. Rupp, and B. Sugg, Fiz. Nizk. Temp. **24**, 281 (1998) [J. Low Temp. Phys. **24**, 212 (1998)].
[24] Z.A. Kazei, P. Novak, and V.I. Sokolov, Zh. Éksp. Teor. Fiz. **83**, 1483 (1982) [Sov. Phys. JETP **56**, 854 (1982)].
[25] S.L. Gnatchenko, V.V. Eremenko, S.V. Sofroneev, N.F. Kharchenko, J.-M. Desvignes, P. Feldmann, and H. Le Gall, Zh. Éksp. Teor. Fiz. 90, 179 (1986) [Sov. Phys. JETP **63**, 102 (1986)].
[26] W. Graeff, J. Kub, and K. Wieteska, Phys. Status Solidi A **126**, 477 (1991).
[27] L.E. Orgel, J. Chem. Phys. **23**, 1004 (1955).
[28] R. Pappalardo, Philos. Mag. **2**, 1397 (1957).